journal

J. Am. Ceram. Soc., 1–8 (2016)
DOI: 10.1111/jace.14079

Properties of Geopolymer Composites Reinforced with Basalt Chopped Strand Mat or Woven Fabric

Daniel Ribero* and Waltraud M. Kriven**,†

Department of Materials Science and Engineering, University of Illinois at Urbana-Champaign, Urbana, Illinois

Geopolymers or polysialates are inorganic polymeric, ceramic-like materials composed of alumina, silica, and alkali metal oxides that can be made without any thermal treatment. Additions of reinforcing phases vastly improve the mechanical properties and high-temperature stability of the geopolymer. The processing and mechanical properties of both chopped strand mat as well as 2-D woven fabric-reinforced potassium geopolymer composites have been evaluated. Hand lay-up and hydraulic press processing methods were used to produce composite panels. The room-temperature tensile and flexural strength of chopped strand mat composites was 21.0 ± 3.1 and 31.7 ± 4.4 MPa, respectively, while those of basalt weave-reinforced geopolymer composites reached 40.0 ± 5.9 and 45.2 ± 9.3 MPa, respectively. Composite microstructures were examined using optical microscopy as well as scanning electron microscopy (SEM). Mass, volume, and porosity fractions were also determined. The effect of high-temperature treatments at 25°C, 300°C, 600°C, and 800°C were analyzed. Finally, Weibull statistical analysis was performed, which showed an increase in reliability when a reinforcement phase was added to K-geopolymer.

I. Introduction

GEOPOLYMERS are a class of amorphous aluminosilicate materials composed of cross-linked alumina (AlO_4) and silica (SiO_2) tetrahedra to form polysialates, with an alkali metal ion to balance the negative charge. They have a faster setting time compared to Ordinary Portland Cement, and have a smaller carbon footprint associated with their production. They also compare very favorably in strength with cements and concretes.[1]

Geopolymers are formed by reacting amorphous metakaolin ($2SiO_2{\cdot}Al_2O_3$) with an alkaline solution of the balancing cation of choice. Previous papers by Kriven et al.[2–5] have shown that a composition with 11 moles of water per mole of 1.2 μm-sized metakaolin allows the majority of the materials to react and polymerize. As such, the composition for this study was therefore fixed at $K_2O \cdot Al_2O_3 \cdot 4SiO_2 \cdot 11H_2O$.

Geopolymers have shown potential as a low-cost, environmentally friendly structural material with the ability to maintain strength at elevated temperatures. They have the advantage of being synthesized as a liquid, allowing them to be cast into any desired shape. Geopolymers have also shown promise as adhesives, bonding strongly to a wide range of ceramics, metals, and when modified, polymers.[6,7] Furthermore, geopolymer can easily be used as a binder system for reinforcements. Musil et al.[4,8,9] and others [10,11] have shown that geopolymer is a good binder for a broad variety of reinforcements, thereby significantly increasing the resulting composite tensile and flexural strength, as compared to pure geopolymer. This property guarantees maximum load transfer from the geopolymer matrix to any reinforcement phase. With properly chosen fiber reinforcement, geopolymer flexural strength can be doubled with as little as 1 wt% addition of 6.35 mm (¼″) chopped basalt fibers.[12] Alternatively, flexural strength can be increased 10-fold with only 10 wt% of 6.35 mm (¼″) chopped basalt fiber additions. Silane sizing has been shown by Rill et al.[12] to produce composites with improved room-temperature flexural strength as compared to those using fibers without sizing.

Moreover, when the geopolymer matrix is heated up to about 350°C–400°C, the water in the geopolymer structure escapes from the bulk of the material, which is accompanied by mechanical deformation and cracking. Since this cracking can often be catastrophic, and while geopolymers otherwise have good high-temperature qualities, it is of high value to research methods of reducing or eliminating this cracking. One of these ways is the addition of a reinforcing phase that vastly improves the mechanical properties and high-temperature stability of the geopolymer.[12]

Basalt is the most common rock found in the earth's crust. Russia has vast and uncalculated basalt reserves, and only the 30 active quarries have roughly 197 million m^3. In the United States, Washington, Oregon, and Idaho have thousands of square miles covered with basalt lava. Basalt is composed (in at.%) primarily of silica and alumina with a nominal composition of 57.5% SiO_2, 16.9% Al_2O_3, 9.5% Fe_2O_3, 7.8% CaO, 3.7% MgO, 2.5% Na_2O, 1.1% TiO_2, and 0.8% K_2O. It has a melting point of 1450 ± 150°C and is noncombustible, making it useful for high-temperature applications. The tensile strength of basalt fiber tends to increase with increasing drawing temperatures, between 1.5 and 2.9 GPa, between 1200°C and 1375°C. Young's modulus of basalt fiber varies between 78 and 90 GPa for basalt fiber from different sources. Compared to glass, most references claim that basalt fiber has higher or comparable elastic modulus and tensile strength.[13–15] Besides their good mechanical properties, basalt fibers have high chemical and thermal stability, as well as good thermal, electrical, and sound insulating properties. The thermal insulating ability of basalt is three times that of asbestos, and due to such good insulating properties basalt is used in fire protection. Basalt has electrically insulating properties which are 10 times better than glass. Secondly, basalt has much better chemical resistance than that of glass fiber, especially in the presence of strong alkalis. Basalt in the form of fibers has been used as a reinforcement phase to geopolymers,[16–20] exhibiting enhancement in mechanical strength compared with pure geopolymer. However, the addition (wt%) of fibers to the geopolymer matrix was limited (up to around 10 wt%) due to rheological problems (shear thickening) beyond that.[4,12]

In this study, potassium-based geopolymer ($K_2O \cdot Al_2O_3 \cdot 4SiO_2 \cdot 11H_2O$) composite panels were produced using

P. Colombo—contributing editor

Manuscript No. 37308. Received August 6, 2015; approved November 17, 2015.
*Member, The American Ceramic Society.
**Fellow, The American Ceramic Society.
†Author to whom correspondence should be addressed. e-mail: kriven@illinois.edu

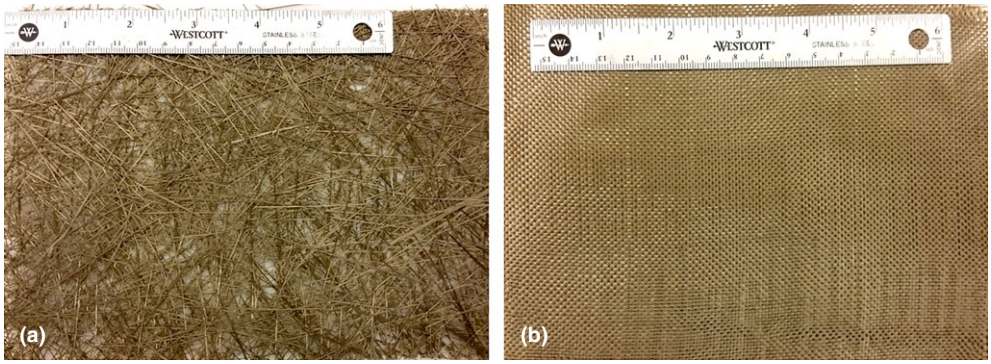

Fig. 1. (a) Chopped basalt strand mat and (b) 2-D basalt plain woven fabric (0°/90°).

Table I. Properties of Basalt Filament, Chopped Strand Mat, and Woven Fabric

Properties	Basalt filaments	Units
Thermal†		
Maximum application temperature	982	(°C)
Sustained operating temperature	820	(°C)
Minimum operating temperature	−260	(°C)
Thermal conductivity	0.031–0.038	(W/mK)
Melting temperature	1450	(°C)
Thermal expansion coefficient	8.0	(ppm/°C)
Physical/Mechanical†		
Density	2.75	(g/cm^3)
Tensile strength	4840	(MPa)
Compressive Strength	3792	(kPa)
Elastic modulus	89	(GPa)
Fabric Properties†		
Weave type	Plain	—
Filament diameter	11	(μm)
Yarn Linear density	100	tex (g/km)
Yarn balance (warp/weft)	1 = (8/ 8)	ends/cm
Density	0.82	(g/cm^3)
Sizing	Silane	—
Mass	0.016	(g/cm^2)
Thickness	0.2	(mm)
Chopped Stand Mat Properties‡		
Density	0.58	(g/cm^3)
Sizing	Silane	—
Mass	350	(g/cm^2)
Thickness	0.6	(mm)

†www.sudaglass.com
‡www.smarter-building-systems.com

chopped strand mat and 2-D basalt woven fabric (0°/90°) (Fig. 1) reinforcement phases (provided by Advanced Filament Technologies, Houston, TX), using hand lay-up and hydraulic press methods. Properties of basalt filaments, plain weave fabric and chopped strand mat reinforcements are shown in Table I. The as-received basalt reinforcements were amorphous and already coated with organic silane-based sizing. Mechanical properties (tensile and flexural) of the geopolymer composite panels were evaluated with reference to failure mechanisms, mass, and volume fractions of the reinforcement phases. Furthermore, the composite structural integrity at elevated temperatures was investigated. These results could shed light on the feasibility of substituting alumina (e.g., Nextel™ 610; 3M Corporation, St. Paul, MN) or mullite-based (e.g., Nextel™ 720; 3M Corporation) reinforcements for intermediate and high-temperature ceramic matrix composite applications.

II. Experimental Procedures

(1) Geopolymer Matrix Preparation

Potassium geopolymer matrix was produced by mixing potassium hydroxide (Sigma-Aldrich, Saint Louis, MO), deionized water, and fumed silica (Cabot, Tuscola, IL) solution (also called potassium "water-glass") with Metamax® metakaolin clay (1.3 μm particle size, BASF, Florham Park, NJ). The proportions were calculated based on the corresponding molar ratios of ($K_2O \cdot Al_2O_3 \cdot 4SiO_2 \cdot 11H_2O$). The slurry was first mixed using an IKA high shear mixer (Model RW20DZM, IKA, Germany), then vibrated on a FMC Syntron vibrating table (FMC Technologies, Houston, TX) to remove trapped air bubbles introduced during the high shear mixing. Additional mixing and degassing was then performed on a Thinky ARE-250 planetary conditioning mixer (Intertronics, Kidlington, Oxfordshire, England). The high shear mixer was run at 1600 rpm for 5 min to produce a low viscosity, homogeneous slurry. The Thinky mixer was run at 1200 rpm for 3 min to further mix, and then 1400 rpm for 3 min to centrifugally de-gas the slurry. This geopolymer preparation procedure has been successfully used to prepare Na-, K-, and Cs-based geopolymers.[3,4,8,9,21] This K-geopolymer matrix was then used to produce composite panels using chopped strand mat and basalt woven fabric reinforcements.

(2) Composite Panel Preparation

Composite panels were prepared using hand lay-up and hydraulic press methods by pouring the geopolymer matrix into 20.32 × 15.24 cm (8 × 6 inch) Delrin® molds (Versatech, LLC, Decatur, IL). Alternating layers of geopolymer and 2-D plain weave basalt fabrics were laid up to produce an eight layer, 0°/90° composite panel. The plain weave and the stacking sequences were not only selected in order to improve the infiltration of the matrix into the reinforcing fabric, but also, to avoid warping or residual stresses during curing. Plain weaves gives both lower fabric weight (g/m^2) as well as fabric cover, than for example satin and twill weaves, which increase the permeability of the fabric. Fabric cover defines the area of 1 cm^2 of a fabric, which is actually covered by warp and weft yarns. Vibration during impregnation of the fabrics reduces the geopolymer viscosity due to its shear thinning behavior and facilitates homogeneous infiltration of the matrix into the fabrics. For chopped strand mat geopolymer composites, five layers were used and the stacking sequence did not matter due to its isotropic nature (randomly oriented 10.16 cm (4″) long fibers). The plates were then covered with a Delrin® top piece, cloth (to absorb expelled geopolymer during pressing) and a steel plate, then held for 24 h at 0.34 MPa (50 psi) in a Carver hydraulic

press. After removal from the press, the composite plates were sealed to avoid dehydration and cured at 50°C for 24 h in a Lab Companion oven (Jeio Tech, Seoul, Korea).

(3) Composites Characterization

The cured panels were 1.6 and 3.2 mm thick for the woven fabric and chopped reinforcements, respectively. Composites were cut into 15.2 mm wide × 148.2 mm long coupons for tensile testing and 10 mm wide × 60 mm long for either three- or four-point flexural testing, using a DrillMaster® 4" tile saw machine (Harbor Freight Tools Co., Camarillo, CA) with a high-speed diamond blade. Tensile test samples were tabbed with G10 fiber glass laminate tabs (fiberglass composite) using Devcon® (ITW Polymers Adhesives, Danvers, MA) two-part epoxy and cured for 24 h prior to testing.

A total of 17 woven fabric (15.2 mm wide × 148.2 mm long × 1.6 mm thick) and 21 chopped strand mat (15.2 mm wide × 148.2 mm long × 3.2 mm thick) reinforced samples were tested under tension at room temperature according to ASTM standard C1275-10,[22] in an Instron load frame (Model 4483, Instron, Norwood, MA) with a 100 KN load cell capacity and an Instron extensometer Model 2630-110 (Instron). The tensile grips used were MTS Advantage Wedge Action Grips, Model 100 (MTS Systems Corp., Eden Prairie, MN). The gauge length was around 100 mm for each sample. Specimens were loaded utilizing a constant displacement rate of 0.02 mm/s. Strain was measured using an extensometer, with a gauge length of 25.4 mm, which was attached so as to be centered on the gage section.

Chopped strand mat-reinforced samples (36 samples) were tested in three-point bending, while woven fabric-reinforced samples (6 for room temperature, 1 for 300°C and 1 for 600°C) were tested on four-point bending using the Instron Universal Testing Frame (Model 5882) with a 50 KN load cell, following ASTM standard C1341-13.[23] In all cases, the sample dimensions were 10 mm wide × 60 mm long x panel thickness. Both three- and four-point flexural testing was performed under displacement control and was set to maintain a strain rate of 1×10^{-3} s^{-1}. The span length between the lower supports was 40 mm and between the upper supports was 20 mm apart being, an equidistant from the point of load application. For room and high-temperature four-point bend testing, samples were mounted in a SiC high-temperature bending apparatus. A 10°C/min ramp rate was used to heat the specimens up to the maximum temperature for high-temperature flexural testing. Samples were held at the maximum temperature for approximately 15 min (at constant strain) to allow for uniform heating inside the sample as well as thermal expansion.

Composite panels as well as post-tested tensile and flexural samples were examined using an optical microscope (Leica Microsystems GmbH, model MZ6, Wetzlar, Germany) and a scanning electron microscope (SEM) (JSM-6060LV, JEOL USA, Inc., Peabody, MA). Samples were put under vacuum for 24 h and Au/Pd sputter coated before analysis, to avoid any outgassing in the SEM.

High-temperature treatments were performed in a box furnace (Carbolite CWF 12/13, Carbolite Inc., Derbyshire, UK) fitted with a Eurotherm 3216 temperature controller. Samples were heat treated (at a ramp rate of ±10°C/min) at maximum temperatures of 300°C, 600°C, and 800°C, without dwell times. After samples had cooled to room temperature, they were weighed to determine the residual mass after the heat treatment.

Fiber mass fraction was calculated using Eq. (1) by determining the area of embedded fabric multiplied by the manufacturer provided, mass per unit area, then dividing by the total sample mass. In the following equations, m and v represent mass and volume fractions while M and V represent overall mass and volume.

$$m_{\text{fiber}} = \frac{l_{\text{specimen}} \cdot w_{\text{specimen}} \cdot M_{\text{fabric per unit area}} \cdot \#\text{ of Plies}}{M_{\text{specimen}}} \quad (1)$$

Fiber volume fraction was calculated in a similar approach by determining the volume of fiber content and dividing it by the total sample volume as seen in Eq. (2), where t is the thickness and ρ is the density. Since the fiber weave was not 100% dense, the fiber volume was calculated by multiplying the volume of the fabric within the sample by the ratio of the fabric density to the solid fiber density.

$$v_{\text{fiber}} = \frac{t_{\text{fabric}} \cdot \frac{\rho_{\text{fabric}}}{\rho_{\text{fiber}}} \cdot \#\text{ of Plies}}{t_{\text{specimen}}} \quad (2)$$

Equations (3) through (6) were used to estimate composite porosity.

$$M_{\text{matrix}} = M_{\text{specimen}}(1 - m_{\text{f}}) \quad (3)$$

$$V_{\text{matrix+pores}} = V_{\text{specimen}}(1 - v_{\text{f}}) \quad (4)$$

$$V_{\text{pores}} = V_{\text{matrix+pores}} - \frac{M_{\text{matrix}}}{\rho_{\text{matrix}}} \quad (5)$$

$$v_{\text{pores}} = \frac{V_{\text{pores}}}{V_{\text{specimen}}} \quad (6)$$

Weibull statistics were also calculated using the maximum tensile and flexural stress data. A distribution function, F, was estimated based on the maximum failure stresses using the median rank method shown in Eq. (7), where the maximum stress for each sample was given a rank, i, (from 1 to n), which is the number of samples in the batch; with a rank of 1 given to the lowest stress value.[24–28]

$$F \cong \frac{i - 0.3}{n + 0.4} \quad (7)$$

The Weibull distribution function is also given by Eq. (8) below, where v is the nondimensional volume, σ is the stress, σ_0 is the scale parameter, and m is the shape parameter or Weibull modulus.

$$F = 1 - e^{[-v(\frac{\sigma}{\sigma_0})^m]} \quad (8)$$

To determine the Weibull parameters, it was assumed that gage length was unchanged in the specimens, so $v = 1$, and Eq. (10) can be rearranged to get Eq. (9) below.

$$\ln[\ln(\frac{1}{1-\text{F}})] = \text{m } \ln(\sigma) - \text{m } \ln(\sigma_0) \quad (9)$$

This fits the common slope-intercept form of a line, so that $\ln[\ln(\frac{1}{1-\text{F}})]$ is then plotted versus $\ln(\sigma)$, using the approximation of F given in Eq. (9), and a linear fit is applied for each data series. The slope of the fit line then corresponds to the Weibull modulus, m, and the y-intercept corresponds to $-m\ln(\sigma_0)$, which can be solved for σ_0. The standard deviation, S, was calculated using Eq. (10) below; where Γ is the Gamma function.

$$S = \sigma_0 \sqrt{\Gamma(1 + \frac{2}{m}) - [\Gamma(1 + \frac{1}{m})]^2} \quad (10)$$

III. Results and Discussion

(1) Physical Properties of Reinforced Geopolymer Composites

Composite panels produced by hand lay-up and hydraulic pressing were homogenous. Geopolymer matrix infiltrated throughout the entire panel thickness and inside fiber bundles

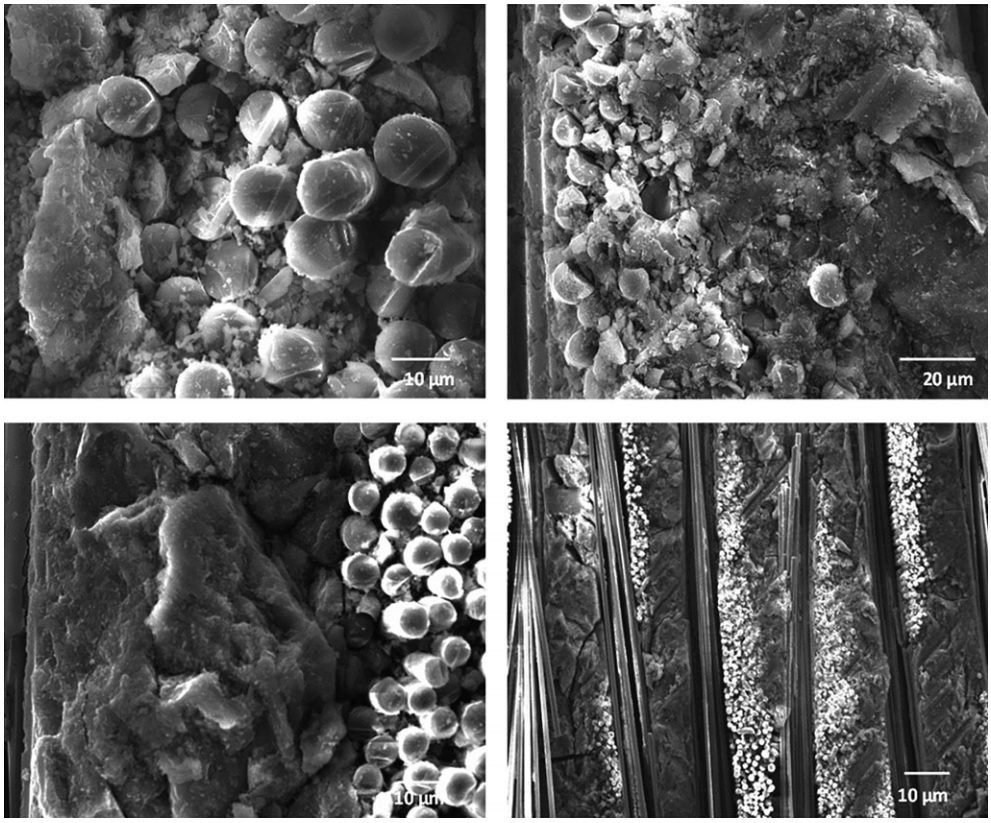

Fig. 2. Woven fabric composite panels produced by hand lay-up and hydraulic pressing.

Table II. Comparative Values of Fiber Mass, Fiber Volume, and Pore Volume Fractions for 2-D Plain Basalt Weave Compared to Chopped Strand Mat, Reinforced K-Geopolymer Composites

Sample	m_f	v_f	v_{pores}
Woven Basalt/KGP	47.3%	29.9%	19.3%
Chopped strand mat/KGP	42.1%	20.6%	28.3%

(Fig. 2) and also showed some adhesion to the basalt fibers thereby allowing for load transfer from the matrix to fiber. This process guaranteed good infiltration, which is required to produce composites with improved and homogeneous properties.

Fiber mass, fiber volume, and pore volume fractions were calculated using Eqs. (1) through (6). Table II present values obtained for 2-D plain weave basalt compared with chopped strand mat, reinforced K-geopolymer composites.

These values for fiber mass fractions were quite high compared with previous research done by Musil et al.,[4] where the reinforcement phase (chopped basalt fibers) was limited to 10 weight percent due to hand mixing processing difficulties at higher fiber contents.

Density determination (mass/volume) and calculation (supplier information) of fabric and strand mat showed that the woven fabric was only about 29% dense while the chopped strand mat was 21% dense, based on the theoretical density of the basalt filament density (2.75 g/cm^3). Composite densities based on mass/volume ratio were found to be 1.71 and 1.35 g/cm^3 for fabric and strand mat composites, respectively. Additionally, composite porosity was calculated as approximately 19% and 28% for fabric and strand mat, respectively. These porosities could be attributed to bubble

Table III. Summary of the Mechanical Properties (Tensile and Flexure) of Pure Geopolymer, Chopped Strand Mat and Woven Fabric Composites

Sample	Test	Scale (σ_0, MPa)	Shape (m)	Standard Deviation (MPa)	95% CI	Scale (σ_0, GPa)	Shape (m)	Standard Deviation (GPa)	95% CI
		Weibull parameters Flexural Strength				Weibull parameters Flexural Modulus			
Pure K-Geopolymer	4-point bending	5.1	2.7	1.8	—	—	—	—	—
Woven Basalt (47 wt%)/KGP	4-point bending	45.2	5.1	9.3	38.3–53.2	13.0	6.1	2.3	11.4–15.0
Chopped Basalt Strand Mat Felt (42 wt%)/KGP	3-point bending	31.7	8.0	4.4	29.6–34.0	4.1	4.7	0.9	3.6–4.6
		Weibull parameters Tensile Strength				Weibull parameters Tensile Modulus			
Pure K-Geopolymer	Tension	1.2	—	—	—	—	—	—	—
Woven Basalt (47 wt%)/KGP	Tension	40.0	7.6	5.9	37.4–42.7	12.2	6.4	2.1	11.2–13.2
Chopped Basalt Strand Mat Felt (42 wt%)/KGP	Tension	21.0	7.4	3.1	19.7–22.3	7.9	7.4	1.2	7.4–8.4

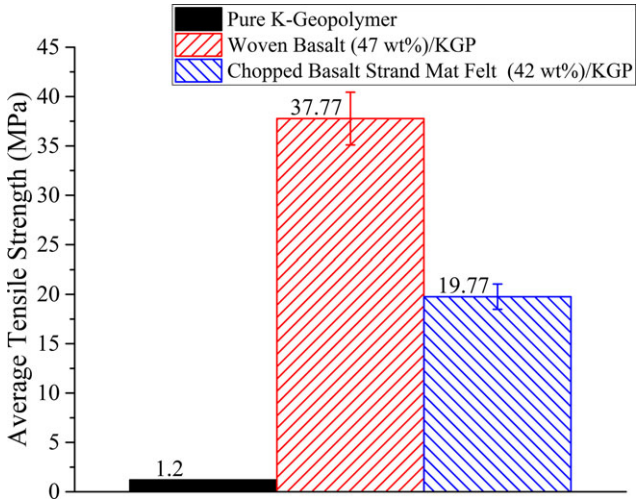

Fig. 3. Average tensile strengths for pure geopolymer, 2-D woven basalt and chopped basalt strand mat composites. The error bars represent the 95% confidence interval (95% CI).

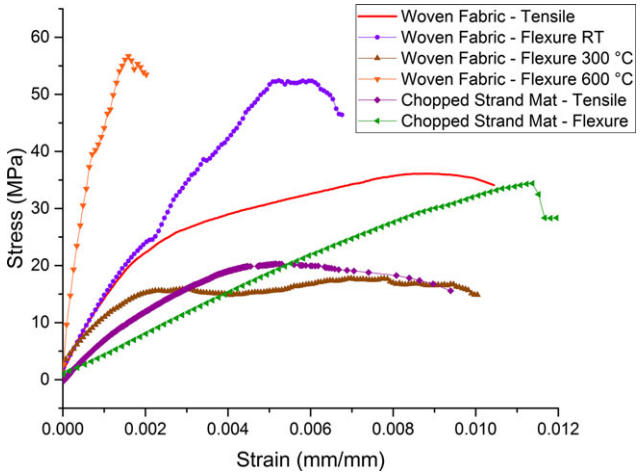

Fig. 4. Typical stress–strain curves for tensile and flexural test.

generation during panel preparation, as well as to degasification during curing and drying of the geopolymer matrix. The amount of pores found in this work were in the same range of porosities found in the literature for reinforced K-geopolymers.[9]

(2) Mechanical Testing of Basalt Reinforced Composites

Table III summarizes the mechanical properties (tensile and flexural) and Weibull statistics of pure geopolymer as well as for the composites made in this investigation. Tensile stress was calculated by dividing the measured tensile load by the sample cross-sectional area. Tensile modulus was determined as the tangent to the tensile stress versus strain curves at a stress value of 5 MPa. The average tensile moduli were calculated as 12.2 ± 2.1 and 7.9 ± 1.2 GPa, for woven fabric and chopped strand mat, respectively. Average tensile strengths for pure geopolymer (1.2 MPa), 2-D woven basalt composites (40.0 ± 5.9 MPa) as well as for, chopped strand mat composites (21.0 ± 3.1 MPa), are plotted in Fig. 3. Typical stress–strain curves for tensile and flexural test are plotted in Fig. 4. For some flexural samples, the stress versus strain curves had to be stopped right after the maximum load because the specimens bent excessively and/or touched the side or bottom of the fixture. In no cases did any sample break completely.

Flexural modulus was determined as the tangent to the flexural stress versus strain curves at a stress value of 3 MPa.

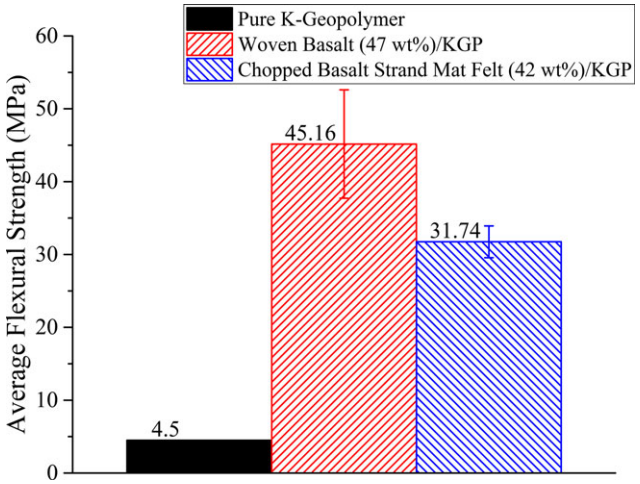

Fig. 5. Average flexural strengths for pure geopolymer, 2-D woven basalt (four-point flexure), and chopped basalt strand mat composites (three-point flexure).. The error bars represent the 95% confidence interval (95% CI).

Average flexural moduli were calculated as 13.0 ± 2.3 and 4.1 ± 0.9 GPa for woven fabric and chopped strand mat, respectively. This behavior represents a significant amount of stiffening over the unreinforced material. Average flexural strengths for pure geopolymer (5.1 ± 1.8 MPa), 2-D woven fabric (45.2 ± 9.3 MPa) and chopped strand mat (31.7 ± 4.4 MPa) composites are plotted in Fig. 5. The error bars for both tensile and flexural strengths were calculated based on the 95% confidence interval (95% CI).

Average tensile and flexural strengths for woven basalt (ranging from 33 times to 8 times) and strand mat (ranging from 17 times to 6 times) composites, respectively, are remarkably higher than for pure geopolymer (1.2 and 5.1 MPa) values. These observations demonstrated the reinforcing effects of the woven fabric and basalt chopped strand mat.

High-temperature flexural results (for woven fabric-reinforced composites) (Fig. 4) showed that at 300°C the flexural strength (17.8 MPa) was reduced by close to half that of the room temperature flexural strength (45.2 MPa). However, at 600°C, the flexural strength was again 56.7 MPa, even higher than at room temperature. This increase in flexural strength at high temperature has been observed also by Musil in Nextel™ 610 alumina-reinforced K-geopolymer composites.[9] Nevertheless, there is no conclusive information that explains this behavior. Some hypotheses such as porosity reduction through glass phase formation, crystallization, and thermal expansion at high temperature, have been proposed. Future work needs to be addressed to clarify the mechanism by which flexural strength is increased at high temperatures.

The results of the Weibull statistical analysis show an increase in reliability over pure geopolymer due to the addition of fiber reinforcement, as seen by the larger values of Weibull modulus. This equates to a higher confidence level of failure at the average tensile and flexural strength values and higher flaw tolerance when compared with pure geopolymer.

(3) Microstructural Characterization

As indicated in Table I, the as-received basalt reinforcements were already coated with organic silane-based sizing. At room temperature, the sizing protects the reinforcements from chemical attack by the highly alkaline geopolymer matrix. Geopolymers do not bond to organics so that the anticipated weak interface is consistent with the enhanced mechanical properties observed.

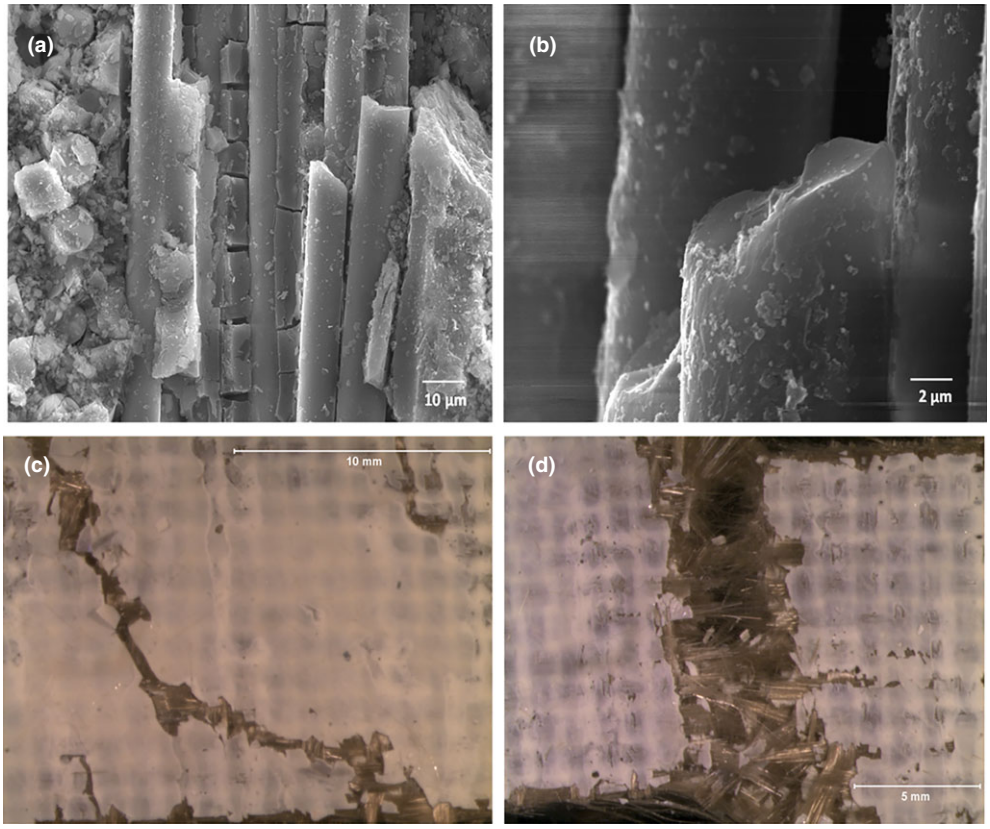

Fig. 6. Failure mechanisms for 2-D woven basalt samples tested in tension: (a) matrix cracking, (b) fiber cracking, (c) crack deflection and (d) fiber pull out.

Table IV. Summary of Residual Mass After Heat Treatment

Sample	Cure temperature	Initial weight (g)	Final weight (g)	Weight percent (%)	Adjusted weight percent (%)
KGP	25	14.66	14.66	100.00	—
	300	16.02	13.75	85.85	—
	600	15.39	10.19	66.21	—
	900	15.07	10.02	66.47	—
Woven Basalt/KGP	25	1.21	1.21	100.00	100.00
	300	1.21	1.19	98.26	96.69
	600	1.49	1.38	92.95	86.63
	800	1.49	1.36	91.81	84.46

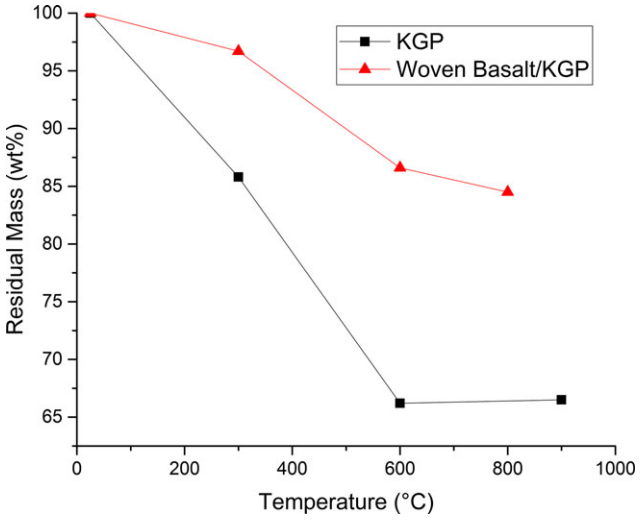

Fig. 7. Average residual mass after heat treatment (No soaking time).

The microstructure of the composites panels produced by hand lay-up and hydraulic pressing is shown in Fig. 2. The panels were homogenous and it was possible to observe that the geopolymer matrix infiltrated throughout the entire panel thickness and within fiber bundles. Furthermore, composites showed some mechanical interlocking of the geopolymer with the basalt fibers, thereby allowing for load transfer from matrix to fiber.

Some failure mechanisms for samples tested in tension are shown in Fig. 6. Crack deflection and fiber pullout were the most common macroscopic composite failure mechanisms found, while fiber and matrix cracking were also microscopic mechanisms detected. Additionally, conchoidal fiber fracture was observed, which is a typical fracture for brittle ceramic materials. For samples tested in flexure, crack deflection, fiber pull out as well as delamination mechanisms were predominant.

(4) Effects of High-Temperature Treatments

When pure geopolymer was cured or heated postcuring, it lost its free water at temperatures up to 400°C. The water removal resulted in dehydration cracking of the material which increased in quantity and severity as heat-treatment temperature increased. As the surface of the geopolymer lost water, capillary forces drew liquid from the interior and created a pressure gradient, which led to cracking and eventual failure in unreinforced samples. The addition of reinforcement phase aided in reducing the severity of the dehydration cracking by bridging the cracks as they developed.

The average residual mass values as a function of heat-treatment temperature are shown in Table IV. The data for 2-D woven basalt composites is compared with that for pure geopolymer and plotted in Fig. 7. The data for the rein-

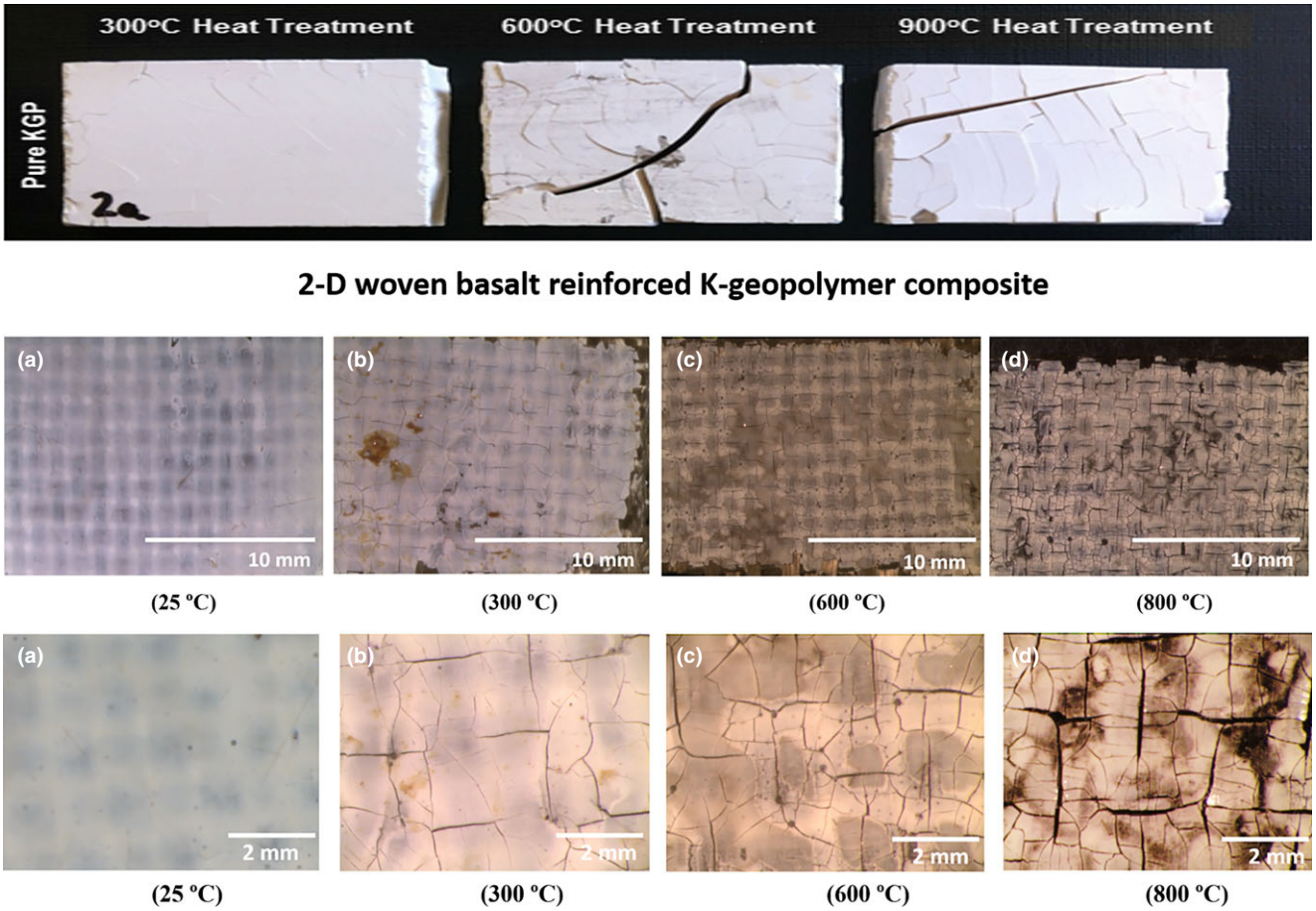

Fig. 8. Optical images of dehydration effects after heat treatment (no soaking time) for pure geopolymer (top row) and 2-D woven basalt composites. (a) 25°C, (b) 300°C, (c) 600°C, and (d) 800°C.

forced composite samples were adjusted to remove the mass of the fiber reinforcement prior to plotting. High-temperature treatment data shows that the reinforced geopolymer actually dehydrated slower and there was less water loss at all temperatures, reaching 84.5 wt% of residual mass at 800°C, compared with about 66 wt% for pure geopolymer. This can be attributed to the additional pathways for water to escape that were created by the fiber matrix interface. These pathways could help to gently dehydrate the geopolymer matrix during curing, reducing pressure gradients through the thickness of the panel and avoiding cracking of the composite.

Figure 8 shows the effect of dehydration on the heat treated samples. As opposed to pure geopolymer that underwent destructive dehydration (complete fracture of the panel), reinforced composites experienced an increase in surface microcracking with increase in temperature, but nevertheless held their structural integrity.

IV. Conclusions

Hand lay-up and hydraulic pressing were successfully used to produce thin homogeneous panels, where there was a good penetration of K-geopolymer matrix through the entire panel thickness and within fiber bundles. This process guaranteed homogeneous geopolymer reaction, as well as uniform mechanical properties throughout the entire panel.

Mass and volume fractions of the reinforcement phase could be increased (compared with chopped fibers) using 2-D basalt fabrics and chopped strand mat, which helped to increase the mechanical strength of the composites. Tensile, three-point and four-point flexural strengths values at room temperature were increased compared with pure geopolymer, for fabric and basalt chopped strand mat-reinforced composites.

An economical and industrial consideration is that the process to produce chopped strand mat is simpler and cheaper than that needed to produce woven fabrics. Therefore, basalt chopped strand mat reinforcements provide a cheaper alternative to basalt fabric reinforcements. The tensile strength loss compared with woven fabric-reinforced composites was about 48%, while for flexural strength was about 30%.

Composites also maintained structural integrity at elevated temperatures and dehydration effects were less destructive than in the pure geopolymer due to fiber bridging. 2-D woven fabric, as well as chopped strand mat basalt geopolymer composites could be used at elevated temperatures (300°C–900°C), using a less expensive reinforcement compared with other ceramic reinforcements such as Nextel™ 610 (alumina fibers) and Nextel™ 720 (mullite). Further extensive research is needed to investigate the increase in flexural strength at 600°C.

Acknowledgments

The authors thank the U.S Air Force Office of Scientific Research (AFOSR), Tyndall Air Force Base, Florida for partially funding this study, under No. FA 9550-06-1-0221. Funding for Daniel Ribero was given by the Sumicol-Corona S.A Company and The National Learning Service of Colombia (SENA). Tensile testing was done at the Mechanical Testing Instructional Laboratory (MTIL) at University of Illinois at Urbana-Champaign under the guidance of Dr. D. Farrow. Scanning electron microscopy was carried out in the Frederick Seitz Materials Research Laboratory, Center for Microanalysis of Materials at the University of Illinois at Urbana-Champaign (which is partially supported by the US Department of Energy under grants DE-FG02-07-ER46453 and DE-FG02-07-ER46471). The authors thank MT. Nick Gencarelle of smarter Building Systems, Newport, RI, for drawing our attention to the basalt reinforcements used in this study.

References

[1]P. Duxson, et al., "Understanding the Relationship Between Geopolymer Composition, Microstructure and Mechanical Properties," *Colloid Surf. A-Physicochem. Eng. Asp*, **269** [1–3] 47–58 (2005).

[2]M. Gordon, J. Bell, and W. M. Kriven, "Comparison of Naturally and Synthetically-Derived, Potassium-Based Geopolymers," *Ceram. Trans.*, **165**, 95–106 (2005).

[3]W. M. Kriven and J. L. Bell, "Effect of Alkali Choice on Geopolymer Properties," *Ceram. Eng. Sci. Proc.*, **25** [4] 99–104 (2004).

[4]S. S. Musil, G. P. Kutyla, and W. M. Kriven, "The Effect of Basalt Chopped Fiber Reinforcement on the Mechanical Properties of Potassium Based Geopolymer"; pp. 31–42 in *Developments in Strategic Materials and Computational Design III: Ceramic Engineering and Science Proceedings*, Vol. **33**. Edited by W. M. Kriven, A. L. Gyekenyesi, G. Westin and J. Wang (Eds.). Wiley, New York, 2013.

[5]W. M. Kriven, J. L. Bell, and M. Gordon, "Microstructure and Microchemistry of Fully-Reacted Geopolymers and Geopolymer Matrix Composites," *Adv. Ceram. Matrix Comp. IX*, **153**, 227–50 (2003).

[6]J. Bell, M. Gordon, and W. Kriven, "Use of Geopolymeric Cements as a Refractory Adhesive for Metal and Ceramic Joins," *Adv. Ceram. Coat. Ceram.-Metal Sys.*, **26** [3] 407–13 (2005).

[7]B. E. Glad, C. Han, W. M. Kriven, and P. Colombo, "Polymer Adhesion to Geopolymer Via Silane Coupling Agent Additives," *J. Am. Ceram. Soc.*, **95** [12] 3758–62 (2012).

[8]S. S. Musil, P. F. Keane, and W. M. Kriven, "Green Composite: Sodium-Based Geopolymer Reinforced With Chemically Extracted Corn Husk Fibers"; pp. 123–33 in *Developments in Strategic Materials and Computational Design IV: Ceramic Engineering and Science Proceedings*, Vol. **34**. Edited by W. M. Kriven, J. Wang, Y. Zhou, A. L. Gyekenyesi, S. Kirihara and S. Widjaja (Eds.). Wiley, Hoboken, 2014.

[9]S. Musil, "Novel, Inorganic Composites Using Porous, Alkali-Activated, Aluminosilicate Binders", Ph. D. Thesis, University of Illinois at Urbana-Champaign, Urbana, IL, (2014).

[10]E. C. Koehler and W. M. Kriven, "Ceramic Felt Reinforced Geopolymer Composites"; in *Developments in Strategic Ceramic Materials II: Ceramic Engineering and Science Proceedings*, Vol. **36**. Edited by W. M. Kriven, J. Wang, D. Zhu, T. Fischer, and S. Kirihara. Wiley, Hoboken, NJ, 2015.

[11]D. S. Roper, G. P. Kutyla, and W. M. Kriven, "Properties of Granite Powder Reinforced Geopolymer Composites"; in *Developments in Strategic Ceramic Materials II: Ceramic Engineering and Science Proceedings*, Vol. **36**. Edited by W. M. Kriven, J. Wang, D. Zhu, T. Fischer, and S. Kirihara. Wiley, Hoboken, NJ, 2015.

[12]E. Rill, D. R. Lowry, and W. M. Kriven, "Properties of Basalt Fiber Reinforced Geopolymer Composites," *Strat. Mater. Comput. Des.*, **31** [10] 57–67 (2010).

[13]R. Parnas, M. Shaw, and Q. Liu, "Basalt Fiber Reinforced Polymer Composites"; The New England Transportation Consortium, Project No. 03-7 - NETCR63 (2007).

[14]V. B. Brik, "Basalt Fiber Composite Reinforcement for Concrete," Transportation Research Board, National Research Council., Contract NCHRP-9 6-IDO25 (1997).

[15]V. T. Ramakrishnan and S. Neeraj, "Performance Evaluation of 3-D Basalt Fiber Reinforced Concrete & Basalt Rod Reinforced Concrete," Transportation Research Board, National Research Council., Contract No. NCHRP-45 (1998).

[16]W. Li and J. Xu, "Mechanical Properties of Basalt Fiber Reinforced Geopolymeric Concrete Under Impact Loading," *Mat. Sci. & Eng.: A*, **505** [1–2] 178–86 (2009).

[17]S. Samal, et al., "Improved Mechanical Properties of Various Fabric-Reinforced Geocomposite at Elevated Temperature," *JOM*, **67** [7] 1478–85 (2015).

[18]M. Welter and M. Schmuecker, "Evolution of the Fibre-Matrix Interactions in Basalt-Fibre-Reinforced Geopolymer-Matrix Composites After Heating," *J. Ceram. Sci. Tech.*, **6** [1] 17–24 (2015).

[19]H. Zhang, V. Kodur, S. Qi, and B. Wu, "Characterizing the Bond Strength of Geopolymers at Ambient and Elevated Temperatures," *Cem. Concr. Compos*, **58**, 40–9 (2015).

[20]R. Davoudian Dehkordi, A. A. Nourbakhsh, and H. MonajatiZadeh, "Investigation of Mechanical Properties of Lithium-Based Geopolymer Composites Reinforced With Basalt Fibers," *J. Adv. Mater. Proc.*, **1** [3] 43–52 (2013).

[21]P. Duxson, S. W. Mallicoat, G. C. Lukey, W. M. Kriven, v. Deventer, and J. S. J, "The Effect of Alkali and Si/Al Ratio on the Development of Mechanical Properties of Metakaolin-Based Geopolymers," *Colloids Surf. A. Physicochem. Eng. Asp.*, **292** [1] 8–20 (2007).

[22]"ASTM C1275-10 Standard Test Method for Monotonic Tensile Behavior of Continuous Fiber-Reinforced Advanced Ceramics With Solid Rectangular Cross-Section Test Specimens at Ambient Temperature".

[23]"ASTM C1341-13 Standard Test Method for Flexural Properties of Continuous Fiber-Reinforced Advanced Ceramic Composites".

[24]W. Weibull, "Statistical Theory of Strength of Materials," *Ingeniors Vetenskaps Akademien – Handlingar*, **151**, 1–45 (1939).

[25]M. H. Dirikolu, A. Aktas, and B. Birgören, "Statistical Analysis of Fracture Strength of Composite Materials Using Weibull Distribution," *Turk. J. Eng. Environ. Sci.*, **26** [1] 45–8 (2002).

[26]C. Lu, R. Danzer, and F. Fischer, "Fracture Statistics of Brittle Materials: Weibull or Normal Distribution," *Phys. Rev. E Stat. Nonlin. Soft. Matter. Phys.*, **65**, 067102, 4pp (2002).

[27]R. Danzer, P. Supancle, J. Pascual, T. Lube, and P. Supancic, "Fracture Statistics of Ceramics – Weibull Statistics and Deviations From Weibull Statistics," *Eng. Fract. Mech.*, **74** [18] 2919–32 (2007).

[28]J. Quinn and G. Quinn, "A Practical and Systematic Review of Weibull Statistics for Reporting Strengths of Dental Materials," *Dent. Mater.*, **26** [2] 135–47 (2010). □